Relativistic spin-polarized calculation of the electronic structure of antiferromagnetic chromium



1992 J. Phys.: Condens. Matter 4 7555

(http://iopscience.iop.org/0953-8984/4/37/003)

J. Phys.: Condens. Matter 4 (1992) 7555–7564. Printed in the UK

# Relativistic spin-polarized calculation of the electronic structure of antiferromagnetic chromium

V Yu Trubitsin, N A Trubitsina and V P Shirokovskii

Physics-Technical Institute, Russia Academy of Sciences, Ural Branch, Kirov Street 132, SU-426001, Izhevsk, Russia

Received 16 March 1992, in final form 20 May 1992

**Abstract.** The electron spectrum and optical absorption of antiferromagnetic chromium are calculated within the relativistic Green function method, being an analogue of the KKR method. The influence of the spin–orbit interaction and the spin polarization on the electron spectrum structure is analysed. An additional optical absorption maximum in the infrared region that is absent in the non-relativistic calculation is shown to appear on the theoretical curve when the relativistic effects are taken into account. The energy positions of this and other maxima due to antiferromagnetic ordering at $\hbar\omega < 0.8$ eV agree well with the experimental data.

## 1. Introduction

Antiferromagnetic ordering in metallic chromium is believed to be directly connected with the Fermi surface topology in the non-magnetic phase. On the basis of a calculation by Wood of the electron spectrum of BCC iron, Lomer [1] has supposed that antiferromagnetic ordering is associated with reciprocal compensation of the electron and hole sheets of the Fermi surface of paramagnetic Cr, centred at the $\Gamma$ and H points of the Brillouin zone (BZ), respectively. The interaction between electrons in the states with the wavevectors $k$ and $k+q$, where $q$ is determined by the distance between the $\Gamma$ and H points of the BZ ($\tilde{q} = (2\pi/a)(1,0,0)$), leads to the formation of an antiferromagnetic gap, which contributes to a lowering of the system energy and ensures the stability of antiferromagnetic ordering. However, as the hole sheet is somewhat larger than the electronic sheet, the maximum compensation occurs for the vectors $\tilde{q} = (2\pi/a)(1-\delta,0,0)$ at $\delta \simeq 0.05$. It is to this fact that Lomer has attributed the spin-density wave (SDW) with the wavevector $\tilde{q}$ incommensurate with the lattice spacing, which has been experimentally observed in antiferromagnetic Cr.

The presence of the SDW makes the calculation of the antiferromagnetic Cr electron spectrum much more complicated. This is why the SDW was neglected in all subsequent *ab initio* calculations. Such an approximation is physically justified by the experimental fact that a state with an SDW is unstable and even with small amounts of alloying additions (e.g. 1% Mn) the SDW disappears. In this case, chromium has a chemical BCC lattice. As the magnetic moments of the atoms located at the corners and in the centre of the cube are equal in magnitude but opposite in direction, the 'magnetic' lattice of antiferromagnetic Cr is simple cubic with a base (i.e. of the CsCl type). Calculations of the electronic structure of antiferromagnetic Cr in such an approximation were performed in [2–5]. In the classical paper by Asano and Yamashita

0953-8984/92/377555+10$04.50  

[2] the calculation was carried out by the self-consistent KKR method using the Slater $X_\alpha$ form to construct the spin-dependent part of the potential. The parameter $\alpha$ was chosen such that the magnetic moment coincides with the experimental value of $0.59\mu_B$. Agreement was obtained at $\alpha = 0.5$, i.e. beyond the range usually considered when calculating within the $X_\alpha$ method. Calculations of the Fermi surface of Cr performed in the same paper confirmed the presumption of Lomer [1] that there is a connection between the SDW and the Fermi surface structure in Cr. The next step in investigating the electronic structure of antiferromagnetic Cr was made by calculations [3–5] performed within the framework of the spin-density-functional theory [6] with the local-spin-density approximation [7]. The LMTO method with the Barth–Hedin exchange–correlation potential [8] was used in [4]. The same potential was chosen in [3], but the functional constants were taken according to Janak [9] (calculations were carried out by the LASW method [10]). As a result, the characteristic dimensions of the electron spectrum in [3] are somewhat greater than in [4], the general structure of the spectrum being the same. Also, Kübler [3] estimated the total energy and the equilibrium value of the lattice constant which proved to be slightly smaller than the experimental value. Nevertheless the magnetic moment for this value coincides with experiment ($0.59\mu_B$). In [4] the magnetic moment for the experimental value of the lattice constant was found to be $0.29\mu_B$. It was also noted that agreement with experiment may be achieved by increasing the lattice constant. Similar results were obtained by Kulikov and Kulatov [5] within the LH KKR method using the Gunnarsson–Lundqvist [11] form.

These studies performed at around the same time almost completed the investigation of the electron spectrum of antiferromagnetic chromium. In more recent papers the main attention was paid to calculations of its physical characteristics. So, the Fermi surface was considered in [12, 13], the change in the Fermi surface under pressure in [5], and the photoemission spectra in [14].

In the last 2–3 years, several papers have been concerned with calculations of the electronic structure of ferromagnetic metals using relativistic spin-polarized methods [15, 16]. It was shown, in particular, that taking into account the spin–orbit interaction together with the spin polarization results in a qualitative change in the electron spectrum. The purpose of the present work is to study the united effect of the spin–orbit interaction and the spin polarization on the electron spectrum structure in antiferromagnetic chromium.

## 2. Computational details

The electron spectrum of antiferromagnetic Cr was calculated by the relativistic version of the Green function method with the spin polarization taken into account (RSPGF). A detailed description of the procedure and the main dispersive equation can be found in [17]. Here we present details of the calculation.

In this paper we used the $l$-dependent model potential of the form

$$V_l^s(r) = (2/r)[[1 + (Z-1)/\{H[\exp(r/d_l^s) - 1] + 1\}]] \qquad (1)$$

($H = d_l(Z-1)^{2/5}$; $d_l$ are the potential parameters having the sense of screening radii; $l$ is the orbital quantum number; $s$ characterizes the spin direction; $Z$ is the nuclear charge).

This model potential was first proposed in [18] to calculate the atomic spectra; subsequently it was used for calculations of the electronic structure of metals. Our experience has shown that such a model potential is convenient to use for calculating physical characteristics of metals with a well known electronic structure. In this case, by fitting the parameters $d_1$, one reconstructs the electron spectrum estimated *ab initio* which is used for further calculations.

As mentioned above, antiferromagnetic Cr has a 'magnetic' lattice of CsCl type. Denoting by 1 and 2 different base atoms in the unit cell, we have the following relations for the potentials at different sites:

$$\begin{aligned} V_l^+(1) &= V_l^-(2) \\ V_l^-(1) &= V_l^+(2). \end{aligned} \tag{2}$$

Thus the total number of parameters in this case amounts to $2l$. (The contributions for $l \leqslant 2$ were taken into account in our calculations.)

The parameters were fitted according to Kübler's [3] calculation performed non-relativistically; so, while fitting the parameters, we had to use the non-relativistic version of the Green function method with spin polarization (SPGF). In passing to the relativistic version (RSPGF) the potential was assumed to be unchanged. The potential parameters used are listed in table 1.

**Table 1.** Parameters $d_l^s$ of the potential (1) for antiferromagnetic Cr.

| $l$ | $d_l^+$ | $d_l^-$ |
|---|---|---|
| 0 | 0.889 | 0.889 |
| 1 | 0.850 | 0.780 |
| 2 | 0.790 | 0.770 |

One more peculiarity of our calculation consists in a lowering of symmetry as a result of taking into account the relativistic effects together with the spin polarization. This can be easily understood from the equation for the large component $\psi$ of the four-component Dirac spinor:

$$\Delta\psi + W[E - (V + \Delta V\,\sigma_z)]\psi - (W'/W)(\boldsymbol{\sigma}\cdot\mathbf{r})(\boldsymbol{\sigma}\cdot\nabla)\psi = 0. \tag{3}$$

Here $\sigma_i$ $(i = x, y, z)$ are the Pauli matrices; $\hat{r}$ is the unit vector;

$$W = 1 + (E - V)/c^2 \tag{4}$$

$c$ is the velocity of light; the prime denotes the derivative with respect to $r$;

$$\begin{aligned} V &= \tfrac{1}{2}(V^+ + V^-) \\ \Delta V &= \tfrac{1}{2}(V^+ - V^-). \end{aligned} \tag{5}$$

Since the last term in (3) remains invariant under any rotation and inversion, the change in symmetry is entirely due to the term $\Delta V\,\sigma_z$ which remains unchanged under rotations about the $z$ axis. In the full cubic symmetry group $O_h$ there are four transformations of this type. Four more transformations are due to the invariance

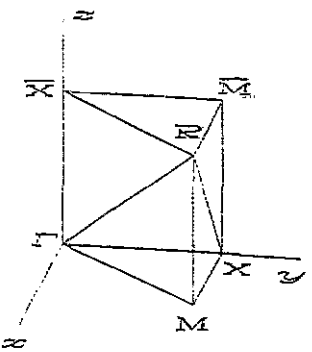


**Figure 1.** One sixteenth of the BZ of a simple cubic lattice.

of equation (3) under rotations changing $z$ into $\bar{z}$ with subsequent translation by the vector $(a/2)(1,1,1)$. Finally, in view of the invariance of the spin under inversion, we obtain eight more symmetry operations. Thus, there are in all 16 symmetry operations which leave equation (3) invariant. Correspondingly, the irreducible part of the BZ is one sixteenth of the full zone (figure 1).

As shown for ferromagnetic Ni and Fe, taking into account the spin polarization together with the relativistic effects results in complete removal of degeneracy. For antiferromagnetic Cr, because of the invariance of equation (3) under sequential operations of time inversion and translation by the vector $(a/2)(1,1,1)$, each state remains doubly degenerate. The general group theoretical considerations of symmetry in relativistic magnetics were reported in [19].

In this paper the electron spectrum of chromium has been calculated at 405 points of one sixteenth of the BZ, which corresponds to 165 points in one forty-eighth of the BZ for a simple cubic lattice.

## 3. Results of calculation

The dispersion curves of the non-relativistic electron spectrum of antiferromagnetic Cr calculated by the SPGF method are presented in figure 2. As the spectrum structure is on the whole similar to that of [3], we shall not dwell upon it. The accuracy of spectrum reconstruction can be estimated by comparing the characteristic widths of the electron spectrum obtained by us and that in [3] (see table 2). One can see from the table that for the points of high symmetry the characteristic values agree to an accuracy of 0.02 Ryd. Since calculations performed within the density-functional theory give a considerably larger spread in energy eigenvalues (see table 2), one can regard the accuracy of the electron spectrum of antiferromagnetic Cr calculated non-relativistically as being good enough; this is also confirmed by the corresponding state density (figure 3).

As seen from figure 4 which presents the dispersion curves of the antiferromagnetic Cr electron spectrum calculated by us within the RSPGF method, taking into account the relativistic effects together with the spin polarization leads to a qualitative change in the whole spectrum structure. The resulting degenerate-level splitting can be estimated from table 3 in which are listed the energy values at the Γ and R points of the BZ for the spin-polarized relativistic and non-relativistic calculations.

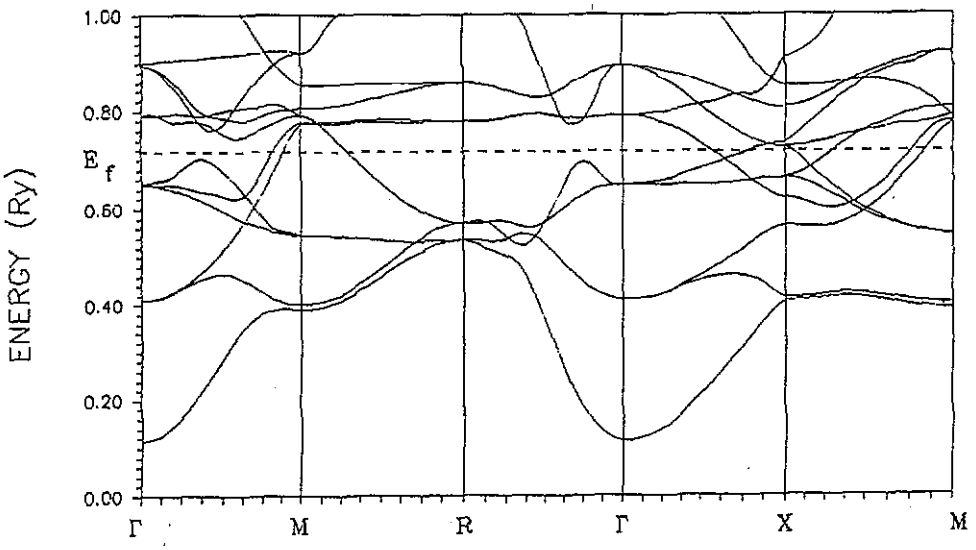


**Figure 2.** Energy bands of antiferromagnetic Cr along the high-symmetry directions: non-relativistic calculation.

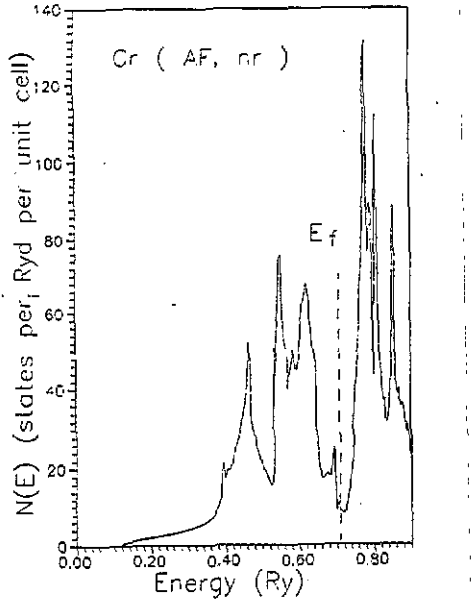


**Figure 3.** Density of states of antiferromagnetic Cr.

If we bear in mind that the general lowering of the spectrum is a manifestation of the mass–velocity and Darwin effects arising in the relativistic theory, the influence of the spin–orbit interaction in antiferromagnetic Cr is seen to be insignificant (the magnitude of splitting does not exceed 2–3 mRyd).

The spin–orbit interaction results not only in splitting of the degenerate states but also in anisotropy of the electron spectrum for the directions $\overline{\Delta}[001]$ and $\Delta[010]$ in the BZ (see figure 1). In the relativistic case these two directions in antiferromagnetic

**Table 2.** Characteristic dimensions of the electron spectrum of antiferromagnetic Cr obtained in various calculations.

| | Energy (Ryd) | | | |
|---|---|---|---|---|
| | Our calculation | Kübler [3] | Kulikov and Kulatov [5] | Asano and Yamashita [2] |
| $\Gamma_{12}$–$\Gamma_1$ | 0.295 | 0.28 | 0.260 | 0.194 |
| $E_F$–$\Gamma_{12}$ | 0.306 | 0.30 | 0.353 | 0.321 |
| $E_F$–$\Gamma_1$ | 0.601 | 0.57 | 0.614 | 0.515 |
| $\Gamma_{25}$–$\Gamma_{12}$ | 0.486 | 0.48 | 0.518 | 0.487 |
| $\Gamma_{12}$–$\Gamma_{25'}$ | 0.142 | 0.15 | | 0.186 |
| $M_3$–$\Gamma_1$ | 0.276 | 0.28 | | 0.203 |
| $M_2$–$M_3$ | 0.385 | 0.39 | | 0.384 |
| $X_2$–$X_1$ | 0.156 | 0.16 | | 0.106 |
| $X_{3'}$–$X_1$ | 0.215 | 0.22 | | 0.215 |
| $R_{15}$–$R_{25'}$ | 0.036 | 0.04 | | 0.021 |
| $R_{12}$–$R_{25'}$ | 0.244 | 0.29 | | 0.244 |
| $R_{25'}$–$\Gamma_1$ | 0.420 | 0.45 | | 0.347 |

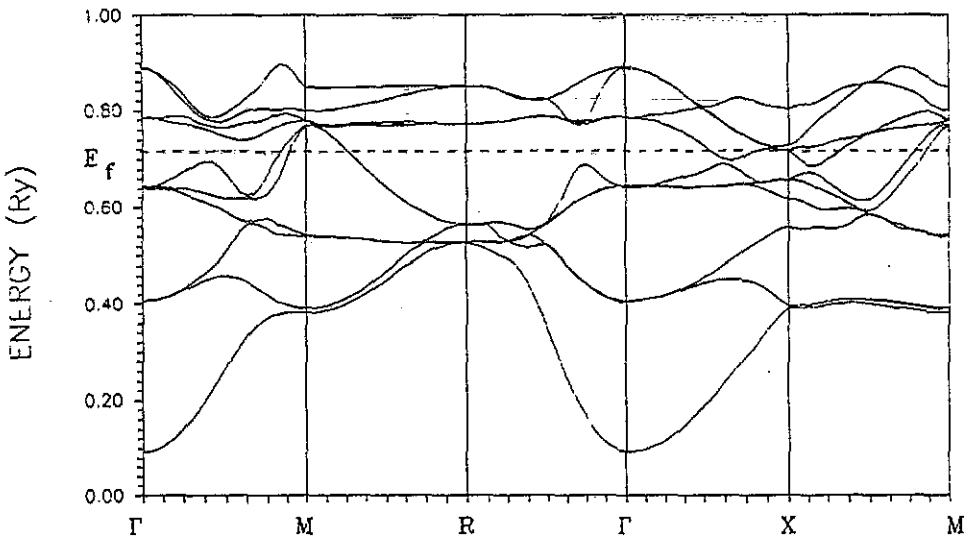


**Figure 4.** Energy bands of antiferromagnetic Cr along the high-symmetry directions: relativistic calculation.

Cr are not equivalent and, correspondingly, the magnitudes of the spin–orbit splitting for the fourfold-degenerate non-relativistic case levels $\Delta_5$ along $\Delta$ and $\overline{\Delta}$ differ. Particular numerical values of the spin–orbit splitting along these directions as well as along T (M–P) and $\overline{T}$ ($\overline{M}$–$\overline{P}$) (see figure 1) are listed in table 4. The anisotropic effect is obviously observed also for other directions and points of the BZ which are equivalent in the non-relativistic calculation and non-equivalent in the relativistic calculation.

By virtue of the smallness of the spin–orbit splitting the main features of the curve of the density of states versus the Fermi energy coincide in the relativistic and non-relativistic calculations of antiferromagnetic chromium, although particular numerical

**Table 3.** Spin–orbit splitting at points Γ and R.

| | Energy $\epsilon(k)$ (Ryd) | |
|---|---|---|
| | Non-relativistic | Relativistic |
| $\Gamma_{12}$ | 0.4094 | 0.40617 |
| | | 0.40618 |
| $\Gamma_{25'}$ | 0.6494 | 0.64283 |
| | | 0.64411 |
| | | 0.64548 |
| $\Gamma_{12}$ | 0.7912 | 0.78520 |
| | | 0.78526 |
| $\Gamma_{25'}$ | 0.8954 | 0.88690 |
| | | 0.88860 |
| | | 0.89031 |
| $R_{25'}$ | 0.5345 | 0.52796 |
| | | 0.52815 |
| | | 0.52852 |
| $R_{15}$ | 0.5700 | 0.56335 |
| | | 0.56385 |
| | | 0.56448 |
| $R_{12}$ | 0.7780 | 0.77151 |
| | | 0.77153 |
| $R_{12'}$ | 0.8576 | 0.85132 |
| | | 0.85134 |

**Table 4.** Anisotropy of the spin–orbit splitting in antiferromagnetic chromium.

| $k_x,k_y,k_z$ $(2\pi/a)$ | $\Delta\epsilon(k)$ (mRyd) | $k_x,k_y,k_z$ $(2\pi/a)$ | $\Delta\epsilon(k)$ (mRyd) | Bands |
|---|---|---|---|---|
| $\Delta(0,\frac{1}{8},0)$ | 1.12 | $\overline{\Delta}(0,0,\frac{1}{8})$ | 1.35 | 5–4 |
| | 2.18 | | 2.32 | 10–9 |
| $\Delta(0,\frac{3}{8},0)$ | 2.33 | $\overline{\Delta}(0,0,\frac{3}{8})$ | 2.62 | 5–4 |
| | 3.33 | | 3.50 | 10–9 |
| X(0,1,0) | 0.02 | $\overline{X}(0,0,1)$ | 3.37 | 6–5 |
| | 0.21 | | 2.73 | 8–7 |
| $T(1,1,\frac{1}{2})$ | 0.34 | $\overline{T}(1,\frac{1}{2},1)$ | 0.00 | 4–3 |
| | 0.28 | | 0.03 | 6–5 |

values of the density of states and the Fermi energy are different. So, the general lowering of the spectrum in the relativistic case results in a change in Fermi energy from 0.710 Ryd in the SPGF calculation to 0.702 Ryd in the RSPGF calculation, and the density of states at the Fermi level increases from 8.84 $Ryd^{-1}$ to 9.65 $Ryd^{-1}$, respectively.

## 4. Optical absorption in antiferromagnetic chromium

The spin–orbit interaction has the most pronounced effect on the optical absorption spectra. The contribution of interband transitions to the optical conductivity of antiferromagnetic Cr has been calculated within the one-electron approximation by the

formula

$$\sigma(\omega) = \frac{4\pi}{3\omega}\frac{1}{\Omega_{WS}}\frac{1}{\Omega_{BZ}}\sum_{ij}\int_{S_{ij}}\frac{|P_{ij}(k)|\,dk}{|\nabla[\epsilon_j(k)-\epsilon_i(k)]|}. \tag{6}$$

Here $\Omega_{WS}$ and $\Omega_{BZ}$ are the volumes of the Wigner–Seitz cell and the BZ respectively; $S_{ij}$ is the surface bounding the reciprocal space area defined by the conditions

$$\begin{aligned}\epsilon_i(k) &\leqslant E_F \leqslant \epsilon_j(k)\\ \epsilon_j(k)-\epsilon_i(k) &\leqslant E\end{aligned} \tag{7}$$

$\epsilon_i(k)$ are the energy eigenvalues for the $i$ band; $P_{ij}$ are the matrix elements of the momentum operator.

Figure 5 shows the results of calculation for the optical absorption of antiferromagnetic Cr in the range from 0 to 0.8 eV. Calculation has been performed in the constant-matrix-element approximation. One can see that taking into account the relativistic effects leads to changes in the magnitude and location of the maxima in the vicinities of 0.16 and 0.45 eV. Also, an additional absorption maximum at 0.37 eV arises which is absent in the non-relativistic calculation. The results obtained are in good agreement with the experimental data. So, in [20] an absorption peak at 0.14 eV and another peak localized in the region of 0.4–0.5 eV were observed. A more detailed measurement of the optical constants of antiferromagnetic Cr performed by the polarimetric method in [21] showed the latter to have a two-hump structure with the maxima localized in the vicinities of 0.38 and 0.48 eV.

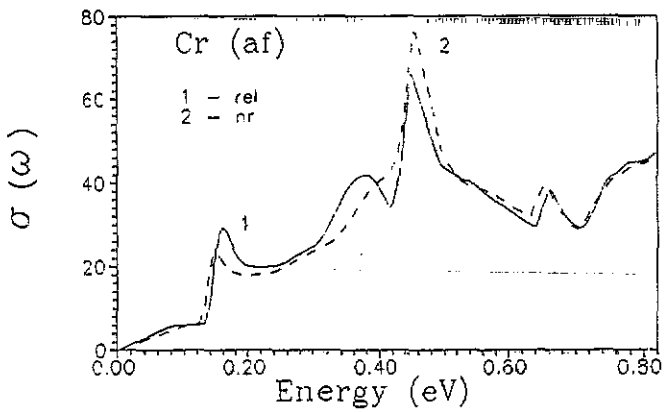


**Figure 5.** Optical absorption edge of antiferromagnetic Cr: ——, relativistic calculation (RSPGF); – – –, non-relativistic calculation (SPGF).

It is seen from the above that the first maximum in our calculation is shifted towards higher energies compared with experiment, the second and the third maxima being shifted to lower energies. This can be explained by the fact that the experimental results [20, 21] have been obtained for pure chromium which has the SDW incommensurate with the lattice spacing, whereas the present calculation is performed for a commensurate SDW. In a paper by Kotani [22] within the framework of the one-dimensional two-band model it was shown that similar shifts of the optical absorption

peaks really occur upon the transition from a state with an incommensurate SDW to a state with a commensurate SDW.

In experiments carried out for alloys in which chromium has a commensurate SDW (Cr–0.94% Mn [20], Cr–Fe [23] and Cr–4% Co [24]), only one optical absorption maximum at 0.46 eV is observed in the infrared region. The absence of a peak at 0.14 eV is attributed to the fact that chromium is in a state with the SDW commensurate with the lattice spacing. Analysis of the results obtained in [23, 24] shows that actually the single peak of optical absorption at 0.46 eV does not exist. Instead in the energy range 0.1–0.8 eV there is a region of elevated optical absorption due to antiferromagnetic ordering. The fine structure of $\sigma(\omega)$ as well as the energy range of elevated absorption itself strongly depend on the type of alloying addition. In our opinion, the experiments performed for the chromium alloys having a commensurate SDW cannot be considered as a reliable criterion for the validity of theoretical calculations. In view of the above, the agreement of the theoretical curve of optical absorption with the experimental data can be regarded as good enough. The optical absorption in antiferromagnetic Cr has been calculated *ab initio* in [25] in the non-relativistic limit. Unfortunately, the fine structure of $\sigma(\omega)$ observed at energies below 0.8 eV is not analysed in detail in this paper. It is only noted that an absorption maximum exists at 0.4 eV, which agrees well with our calculation.

## 5. Conclusion

The calculation performed has shown that with the relativistic effects taken into account the symmetry of problem changes, which results in a total change in the electron spectrum structure in collinear antiferromagnets. In particular, the spin–orbit interaction leads to the splitting of all energy levels degenerate in the non-relativistic version. Although in antiferromagnetic chromium this splitting is small, particular values of such integral characteristics as density of states and optical absorption substantially change. Moreover, for the optical absorption in the infrared region to be correctly interpreted, the relativistic effects must necessarily be taken into account.

## References

[1] Lomer W M 1962 *Proc. Phys. Soc.* **86** 489
[2] Asano S and Yamashita J 1967 *J. Phys. Soc. Japan* **23** 714
[3] Kübler J 1980 *J. Magn. Magn. Mater.* **20** 277
[4] Skriver H L 1980 *J. Phys. F: Met. Phys.* **11** 97
[5] Kulikov N I and Kulatov E T 1982 *J. Phys. F: Met. Phys.* **12** 2291
[6] Kohn W and Sham L J 1965 *Phys. Rev.* A **140** 1133
[7] Hedin L and Lundqvist B I 1965 *J. Phys. C: Solid State Phys.* **4** 2064
[8] Barth H and Hedin L 1972 *J. Phys. C: Solid State Phys.* **5** 1629
[9] Janak J F 1978 *Solid State Commun.* **25** 53
[10] Williams A R, Kübler J and Gelatt C D 1979 *Phys. Rev.* B **19** 6094
[11] Gunnarsson O and Lundqvist B I 1976 *Phys. Rev.* B **13** 4274
[12] Singh A K, Mannel A A and Walker E 1988 *Europhys. Lett.* **6** 67
[13] Fry J L, Brener N E, Laurent D G and Callaway J 1981 *J. Appl. Phys.* **52** 2101
[14] Komeda T *et al* 1989 *Phys. Rev.* B **39** 6198
[15] Ebert H, Strange P and Gyorffy B 1988 *J. Phys. F: Met. Phys.* **18** L135
[16] Shadler G, Weinberger P, Boring A M and Albers R C 1986 *Phys. Rev.* B **34** 713
[17] Ostanin S A and Shirokovskii V P 1991 *J. Phys.: Condens. Matter* **3** 5287

[18] Green A E S, Sellin D L and Zachor A S 1969 *Phys. Rev.* **184** 1
[19] Hormandinger G and Weinberger P 1992 *J. Phys.: Condens. Matter* **4** 2185
[20] Bos L W and Lynch D W 1970 *Phys. Rev.* **2** 4567
[21] Ganin G V, Kirillova M M, Nomerovannaya L V, Shirokovskii V P 1977 *Fiz. Metall. Metalloved.* **43** 907
[22] Kotani A 1974 *J. Phys. Soc. Japan* **34** 1493
[23] Kirillova M M and Nomerovannaya L V 1975 *Fiz. Metall. Metalloved.* **40** 983
[24] Nomerovannaya L V, Kirillova M M, Kozhevnikova M V 1976 *Fiz. Metall. Metalloved.* **42** 732
[25] Kulikov N I, Alouani M, Khan M A, Magnitskaya M V 1987 *Phys. Rev.* B **36** 929